Electrophoretic and Dielectrophoretic Field Gradient Technique for Separating Bioparticles

Michele D. Pysher and Mark A. Hayes*

Department of Chemistry and Biochemistry and Arizona Applied NanoSensors, Arizona State University, P.O. Box 871604, Tempe, Arizona 85287-1604

We describe a new device for separation of complex biological particles and structures exploiting many physical properties of the biolytes. The device adds a new longitudinal gradient feature to insulator dielectrophoresis, extending the technique to separation of complex mixtures in a single channel. The production of stronger local field gradients along a global gradient allows particles to enter, initially transported through the channel by electrophoresis and electroosmosis, and to be isolated according to their characteristic physical properties, including charge, polarizability, deformability, surface charge mobility, dielectric features, and local capacitance. In this work, the separation mechanism is described in terms of the relevant electromechanical principles, and proof-of-principle is demonstrated using various bacteria cells as model systems. The results demonstrate the selectivity of the technique and suggest that it may form the foundation for a versatile and useful tool for separating mixtures of complex biological particles and structures.

The separation of biological particles and structures is a formidable task. In addition to the typical difficulties inherent to analytical separations, the process is often further complicated by the physical and chemical heterogeneity and complexity of both the particles and the sample matrix. For instance, diagnostic and therapeutic cellular analysis frequently requires isolating components from samples containing numerous cell types in various stages of development. The methods employed can vary greatly depending on the specific nature of the sample and the desired outcome. Bulk techniques such as centrifugation and affinity-based filtration and cell sorting are common choices for preparative steps or high throughput applications. For more demanding applications requiring higher purity from smaller samples, electric field-based techniques are particularly attractive because of their high-resolution and efficiency.

Several strategies have been explored and developed for separating bioparticles. One method that enables the charge-based separation of suspended particles is capillary electrophoresis (CE). This method has been used to separate and characterize a variety of biological and biomimetic structures including liposomes,[1−5] bacteria,[6−8] subcellular components,[9] and mammalian cells.[10] Moreover, research in buffer additives and specialized surface coatings has continued to increase the applicability of these systems. While CE has proven very useful for some applications, several shortcomings have also been noted. For example, mixtures of different cell types or live and dead cells could not always be successfully separated.[6−8] In addition to traditional CE methods, some groups have reported enhanced selectivity using hybrid techniques such as radial migration and isoelectric focusing.[11−15]

Dielectrophoresis (DEP) has found widespread use as well. DEP exploits the force exerted by a nonuniform electric field on a polarizable particle.[16−22] In general terms, it occurs as a result of the force exerted by the external field on the field-induced dipole moment of the polarized particle. The DEP effect was first described by Pohl in his landmark 1951 publication, which presented a theoretical explanation for the phenomena and reported on its use for removing suspended particles from polymer solutions.[20,21] Since then DEP has been adapted and applied to a wide variety of biological structures such as cells, spores, bacteria,

* Corresponding author. E-mail: mhayes@asu.edu. Office: 480-965-2566. Fax: 480-965-2747.

(1) Duffy, C. F.; Gafoor, S.; Richards, D. P.; Admadzadeh, H.; O Kennedy, R.; Arriaga, E. A. *Anal. Chem.* **2001**, *73*, 1855−1861.
(2) Owen, R. L.; Strasters, J. K.; Breyer, E. D. *Electrophoresis* **2005**, *26*, 735−751.
(3) Pysher, M. D.; Hayes, M. A. *Langmuir* **2005**, *21*, 3572−3577.
(4) Pysher, M. D.; Hayes, M. A. *Langmuir* **2004**, *20*, 4369−4375.
(5) Radko, S. P.; Stastna, M.; Chrambach, A. *Anal. Chem.* **2000**, *72*, 5955−5960.
(6) Armstrong, D. W.; Girod, M.; He, L. F.; Rodriguez, M. A.; Wei, W.; Zheng, J. J.; Yeung, E. S. *Anal. Chem.* **2002**, *74*, 5523−5530.
(7) Armstrong, D. W.; Schneiderheinze, J. M. *Anal. Chem.* **2000**, *72*, 4474−4476.
(8) Armstrong, D. W.; Schulte, G.; Schneiderheinze, J. M.; Westenberg, D. J. *Anal. Chem.* **1999**, *71*, 5465−5469.
(9) Duffy, C. F.; Fuller, K. M.; Malvey, M. W.; O Kennedy, R.; Arriaga, E. A. *Anal. Chem.* **2002**, *74*, 171−176.
(10) Mehrishi, J. N.; Bauer, J. *Electrophoresis* **2002**, *23*, 1984−1994.
(11) Kennedy, R. T.; Oates, M. D.; Cooper, B. R.; Nickerson, B.; Jorgenson, J. W. *Science* **1989**, *246*, 57−63.
(12) Lu, H.; Gaudet, S.; Schmidt, M. A.; Jensen, K. F. *Anal. Chem.* **2004**, *76*, 5705−5712.
(13) McClain, M. A.; Culbertson, C. T.; Jacobson, S. C.; Ramsey, J. M. *Anal. Chem.* **2001**, *73*, 5334−5338.
(14) Witek, M. A.; Wei, S. Y.; Vaidya, B.; Adams, A. A.; Zhu, L.; Stryjewski, W.; McCarley, R. L.; Soper, S. A. *Lab-on-a-Chip* **2004**, *4*, 464−472.
(15) Zheng, J. J.; Yeung, E. S. *Anal. Chem.* **2003**, *75*, 3675−3680.
(16) Jones, T. B. *J. Electrostat.* **1979**, *6*, 69−82.
(17) Jones, T. B. *J. Electrostat.* **1986**, *18*, 55−62.
(18) Jones, T. B. *Electromechanics Particles*; Cambridge University Press: New York, 1995.
(19) Jones, T. B.; Washizu, M. *J. Electrostat.* **1996**, *37*, 121−134.
(20) Pohl, H. A. *Dielectrophoresis*; Cambridge University Press: Cambridge, 1978.
(21) Pohl, H. A. *J. Appl. Phys.* **1951**, *22*, 869−871.
(22) Washizu, M.; Jones, T. B. *J. Electrostat.* **1994**, *33*, 187−198.

10.1021/ac070534j CCC: $37.00
Published on Web 05/08/2007

and viruses.[23−27] Unlike CE, which depends primarily on the charge-to-size ratio of the particle, DEP depends on a rich set of both structural and chemical properties. Because of this, enhanced selectivity and sensitivity are often realized. Through its use, researchers have achieved impressive results including separating cancer cells from blood cells,[23,28,29] parasitized cells from normal cells,[24,26,28−39] and live from dead cells.[31]

While DEP has proven to be a highly selective and versatile technique, it also has several inherent limitations. One limitation is the electrodes embedded within the separation chamber which are used to establish the required nonuniform electric fields. These can cause undesirable electrochemical reactions and gas generation at the surfaces of these electrodes. Although the use of AC rather than DC voltage helps to minimize these effects, it does not eliminate them. Traditional DEP devices are also generally limited to separating two distinctly different components, one that collects in the high field strength regions (typically located on, or near, the electrodes) and one that does not. Consequently, separating particles with similar properties requires optimizing the specific experimental parameters, such as buffer conductivity, field strength, and frequency. Various techniques have emerged in response to these limitations.[40−46] For instance, single cell manipulation has been demonstrated using methods and devices based on three-dimensional arrays of microelectrodes or field cages,[41,47] while others have reported achieving increased efficiency and greater control over particle transport through the use of individually addressable or programmable electrodes.[40,43]

More recently, insulator-based dielectrophoresis (DC-iDEP) has emerged.[48] This method differs from traditional DEP in that a DC voltage is applied to electrodes located in remote inlet and outlet reservoirs, and the field nonuniformities are generated by arrays of insulating posts located within the channel. Cummings and Singh described the theoretical basis of the technique and demonstrated proof-of- principle using latex spheres.[48] In subsequent studies, the technique was used to concentrate and isolate live and dead bacteria,[49,50] similar to what is presented here, except this new strategy allows the longitudinal separation of mixtures as opposed to a simply bifurcation of two components. Geometric shapes were exploited for bacteria separation from latex particles.[51] DC-iDEP offers several advantages compared to traditional DEP. The use of remote electrodes avoids many of the problems associated with embedded electrodes, such as electrochemical reactions and gas generation at the electrode surfaces. Additionally, the field can be generated by applying DC rather than AC voltage. Use of a DC field can be advantageous because it can be used to drive both electrophoretic and dielectrophoretic transport, allowing greater control over particle movement.

In this report, we describe a new DC-iDEP-based separation device and demonstrate proof-of- principle using various bacteria as model systems. The technique produces sequential, spatially resolved separations by simultaneously exploiting electrophoretic, electroosmotic, and dielectrophoretic transport mechanisms. Electrophoresis and electroosmosis are used to transport the particles through a channel containing a series of progressively stronger field gradient regions. As the particles are transported through the channel, they are isolated according to their characteristic physical properties in response to electrophoretic and dielectrophoretic forces. Because this technique relies on both electrophoretic and dielectrophoretic forces, it accesses a much richer set of properties to accomplish separation than many other techniques. Furthermore, the incorporation of electrophoretic transport mechanisms allows for greater control over sample introduction and particle movement, and faster separations.

EXPERIMENTAL SECTION

Cells. *Bacillus subtilis*, *Escherichia coli*, and *Staphylococcus epidermidis* were obtained from American Type Culture Collection (Manassas, VA). Bacteria cultures were grown on nutrient agar or in LB broth to log phase following standard protocols recommended by the supplier. Prior to fluorescent staining the cells were harvested and suspended in 0.85% NaC1. Cells were stained using a two-color fluorescence assay BacLight Kit Ll3l52 (Molecular Probes, Eugene, OR) according to the suggested protocols. The assay utilizes Syto 9 and propidium iodide to stain live cells fluorescent green and dead cells fluorescent red. The reported excitation/ emission characteristics for these dyes are 480/500

(23) Becker, F. F.; Wang, X. B.; Huang, Y.; Pethig, R.; Vykoukal, J.; Gascoyne, P. R. C. *Proc. Natl. Acad. Sci. U.S.A.* **1995**, *92*, 860−864.
(24) Gascoyne, P.; Mahidol, C.; Ruchirawat, M.; Satayavivad, J.; Watcharasit, P.; Becker, F. F. *Lab-on-a-Chip* **2002**, *2*, 70−75.
(25) Gascoyne, P. R. C.; Vykoukal, J. *Electrophoresis* **2002**, *23*, 1973−1983.
(26) Green, N. G.; Morgan, H. *Journal Of Physics D-Applied Physics* **1998**, *31*, L25−L30.
(27) Green, N. G.; Morgan, H.; Milner, J. J. *J. Biochem. Biophys. Methods* **1997**, *35*, 89−102.
(28) Huang, Y.; Ewalt, K. L.; Tirado, M.; Haigis, R.; Foster, A.; Ackley, D.; Heller, M. J.; O Connell, J. P.; Krihak, M. *Anal. Chem.* **2001**, *73*, 1549−1559.
(29) Huang, Y.; Wang, X. B.; Becker, F. F.; Gascoyne, P. R. C. *Biochim. Biophys. Acta-Biomembranes* **1996**, *1282*, 76−84.
(30) Green, N. G.; Morgan, H.; Milner, J. J. *J. Biochem Biophys. Methods* **1997**, *35*, 89−102.
(31) Markx, G. H.; Talary, M. S.; Pethig, R. *J. Biotechnol.* **1994**, *32*, 29−37.
(32) Morgan, H.; Green, N. G. *J. Electrostat.* **1997**, *42*, 279−293.
(33) Morgan, H.; Hughes, M. P.; Green, N. G. *Biophys. J.* **1999**, *77*, 516−525.
(34) Pethig, R. *Crit. Rev. Biotechnol.* **1996**, *16*, 331−348.
(35) Pethig, R.; Huang, Y.; Wang, X. B.; Burt, J. P. H. *J. Phys. D: Appl. Phys.* **1992**, *25*, 881−888.
(36) Ramos, A.; Morgan, H.; Green, N. G.; Castellanos, A. *J. Phys. D: Appl. Phys.* **1998**, *31*, 2338−2353.
(37) Wang, X. B.; Huang, Y.; Burt, J. P. H.; Markx, G. H.; Pethig, R. *J. Phys. D-Appl. Phys.* **1993**, *26*, 1278−1285.
(38) Wang, X. B.; Huang, Y.; Gascoyne, P. R. C.; Becker, F. F.; Holzel, R.; Pethig, R. *Biochim. Biophys. Acta-Biomembranes* **1994**, *1193*, 330−344.
(39) Gascoyne, P.; Pethig, R.; Satayavivad, J.; Becker, F. F.; Ruchirawat, M. *Biochim. Biophys. Acta-Biomembranes* **1997**, *1323*, 240−252.
(40) Cheng, J.; Sheldon, E. L.; Wu, L.; Heller, M. J.; O Connell, J. P. *Anal. Chem.* **1998**, *70*, 2321−2326.
(41) Durr, E.; Yu, J. Y.; Krasinska, K. M.; Carver, L. A.; Yates, J. R.; Testa, J. E.; Oh, P.; Schnitzer, J. E. *Nat. Biotechnol.* **2004**, *22*, 985−992.
(42) Fiedler, S.; Shirley, S. G.; Schnelle, T.; Fuhr, G. *Anal. Chem.* **1998**, *70*, 1909−1915.
(43) Hunt, T. P.; Lee, H.; Westervelt, R. M. *Appl. Phys. Lett.* **2004**, *85*, 6421−6423.
(44) Minerick, A. R.; Zhou, R. H.; Takhistov, P.; Chang, H. C. *Electrophoresis* **2003**, *24*, 3703−3717.
(45) Wang, X. B.; Huang, Y.; Wang, X. J.; Becker, F. F.; Gascoyne, P. R. C. *Biophys. J.* **1997**, *72*, 1887−1899.
(46) Wong, P. K.; Chen, C. Y.; Wang, T. H.; Ho, C. M. *Anal. Chem.* **2004**, *76*, 6908−6914.
(47) Fiedler, S.; Shirley, S. G.; Schnelle, T.; Fuhr, G. *Anal. Chem.* **1998**, *70*, 1909−1915.
(48) Cummings, E. B.; Singh, A. K. *Anal. Chem.* **2003**, *75*, 4724−4731.
(49) Lapizco-Encinas, B. H.; Simmons, B. A.; Cummings, E. B.; Fintschenko, Y. *Anal. Chem.* **2004**, *76*, 1571−1579.
(50) Lapizco-Encinas, B. H.; Simmons, B. A.; Cummings, E. B.; Fintschenko, Y. *Electrophoresis* **2004**, *25*, 1695−1704.
(51) Barrett, L. M.; Skulan, A. J.; Singh, A. K.; Cummings, E. B.; Fiechtner, G. J. *Anal. Chem.* **2005**, *77*, 6798−6804.

nm for Syto 9 and 490/635 nm for propidium iodide, allowing the simultaneous observation of both live and dead cells through a standard wide-band blue filter set. After staining, the cells were resuspended in 1 mM phosphate buffer pH 7.6 for use.

Device Fabrication. The microfluidic devices were fabricated using standard photolithography, fabrication, and bonding techniques. Devices were fabricated from Schott D263 glass wafers (S. I. Howard Glass Company, Worcester, MA) and PDMS. The photomasks were designed in-house using AutoCAD (Autodesk, Inc., San Rafael, CA) and printed as photoplots.

Devices were fabricated both completely from glass and from PDMS with a glass cover plate. Both designs produced acceptable results; however, during our studies the PDMS/glass devices were found to be preferable for several reasons: (1) The profile of etched glass channels are distorted due to anisotropic etching; however, the channel wall profile is maintained when fabricated from PDMS. (2) Bacterial adhesion and fouling of the devices occurred less often. (3) The fabrication process is easier, less costly, and takes considerably less time.

The devices were fabricated following previously established procedures. Briefly, the PDMS portion of the device was fabricated using channel molds fabricated from resists using standard photolithography techniques. Access holes were made using a hole punch, and then the PDMS channel was sealed to a glass cover plate by plasma oxidation, followed by contact sealing.

Separations and Data Collection. The separations were monitored using an inverted fluorescence microscope (Olympus IX70) equipped with a QICAM ccd camera (Q Imaging Inc.). Images were captured using Stream Pix III (version 3.6.0, Norpix) data capture program.

Channel Designs. All channel depths are 20 μm, and the maximum channel widths are 500 μm. The initial tooth height (base to tip) of channel A is 150 μm, and the width (across base) is the same as the height, 150 μm. Their heights and widths increase in 10 μm increments after every third tooth in the series. The final tooth height (last three teeth) is 240 μm and the width is also 240 μm. For channel B, the initial tooth height (base to tip) is 100 μm and the width (across base) is twice the height, or 200 μm. Their heights increase in 5 μm increments after every third tooth in the series (and widths increase in 10 μm increments). The final tooth height (last three teeth) is 240 μm and the width is 480 μm. For channel C, the initial tooth height (base to tip) is 100 μm and the width (across base) is twice the height, or 200 μm. Their heights increase in 5 μm increments (and widths in 10 μm increments) after each tooth in the series. The final tooth height (last tooth) is 240 μm and the width is 480 μm.

Safety Considerations. All bacteria species used in this study were classified as Bio Safety Level 1 (BSL1) and were handled according to the recommended guidelines for BSL1 organisms.

RESULTS AND DISCUSSION

There is considerable interest in developing efficient, high-resolution techniques for separating mixtures of complex biological particles and structures. Much of the recent work reported has focused on developing electric field-based microfluidic techniques. These devices are particularly attractive due to their high separation efficiencies, short analysis times, and minimal sample consumption. Most of the currently employed methods rely on either electrophoretic or dielectrophoretic forces; however, enhanced efficiency and specificity can be achieved by utilizing the effects of both forces. Here, we describe a technique that exploits the effects of both electrophoretic and dielectrophoretic forces growing out of the pioneering work on insulator dielectrophoresis. In this section, we first describe the technique in terms of the relevant electromechanical forces, a brief review of the fundamental principles and theories, and then present experimental results demonstrating proof-of-principle.

Fundamental Principles and Electromechanics. A suspended particle subjected to a spatially nonuniform electric field experiences electrical forces that can cause both electrophoresis and dielectrophoresis (DEP),[16−21,34,36] along with accompanying electroosmotic actions. Electrophoretic forces are well chronicled and generally result from the frictional forces balancing electric field forces. For the DEP, the translational force can cause motion toward increasing local field strength (positive DEP) or decreasing field strength (negative DEP). The total electrical force (F) exerted on a particle can be estimated by the sum of the electrophoretic and dielectrophoretic forces it experiences. For the simplified case of a homogeneous spherical particle, this total force can be approximated by:

$$F = qE + \pi 2\epsilon_m r^3 \alpha \nabla E^2 \quad (1)$$

where the first term represents the electrophoretic force and the second the dielectrophoretic force.[16−21,34,36] In the above equation, E is the electric field strength, ϵ_m is the permittivity of the suspending medium, q is the effective net charge, and r the radius of the particle. The factor ∇E^2 (the gradient of the square of the field) quantifies both the magnitude and spatial nonuniformity of the local field. The Clausius−Mossotti factor (α) is a parameter defining both the magnitude and direction of the field-induced dipole moment. It reflects the effective polarizability of the particle with respect to the medium. In the low-frequency or DC limit, which is governed by conduction effects, the Clausius−Mossotti factor can be approximated by its real (in phase) component given by:

$$\alpha = \frac{\sigma_p - \sigma_m}{\sigma_p - 2\sigma_m} \quad (2)$$

where σ_p and σ_m are the real conductivities of the particle and medium respectively. Positive DEP (movement toward field maxima) occurs if a particle is more polarizable than the medium ($\alpha > \sigma$), whereas negative DEP (movement toward field minima) occurs if a particle is less polarizable ($\alpha < \sigma$).

General Design Principles and Description of Technique. The devices were designed according to DC-iDEP principles. Unlike traditional DEP systems that utilize embedded electrodes and AC fields to generate the necessary field gradients, here a DC voltage is applied and the field nonuniformities are generated by the channel walls. Because the walls are nonconducting, the applied field is confined within them. Consequently, the local properties (magnitude and gradient) of the field are defined by the morphology of the channel. When a DC voltage is applied to a typical, smooth-walled fluidic channel of fixed width, a uniform electric field is generated throughout the channel. Conversely, if

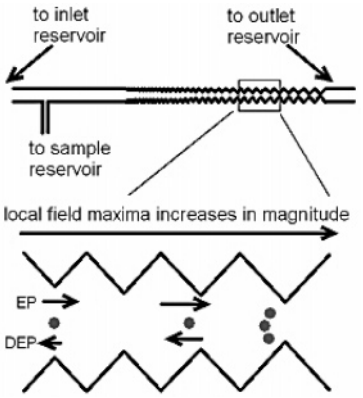

Figure 1. Schematic showing a representative channel design (upper) and a graphical depiction of the particle trapping mechanism (lower). The strength of the field gradient traps increases in the direction of the outlet (left to right). Particle trapping by negative DEP is shown. As a particle approaches the local field maxima in each successive field gradient trap, the DEP force it experiences increases. If the electrophoretic forces it experiences at a local field maximum are greater than the DEP force, the particle will pass by that trap and continue through the channel. When a particle reaches a trap of sufficient strength that the DEP force becomes greater than the electrophoretic forces, the particle becomes immobilized.

the width of the channel does not remain fixed, the local magnitude of the field will be larger in narrower areas of the channel and smaller in wider areas, thus creating regions of nonuniformity, or field gradients.

A schematic of a representative device and graphical depiction of the separation and trapping mechanism are shown in Figure 1. For these studies, the series of field gradient regions was created by designing the channel walls in a 'saw-tooth' pattern. Each pair of opposing teeth establishes a local gradient region that acts as separate dielectrophoretic trap; the local field maxima are located at the tips of the teeth and the minima at their base. The physical parameters of the teeth (including width, height, angle, and proportions) determine the strength of each trap (defined by the local gradient and magnitude of the field within it). Therefore, gradient regions, or dielectrophoretic traps, of differing strengths can be created by varying the physical parameters of the teeth throughout the device. Here, the devices were designed so that a series of dielectrophoretic traps of gradually increasing strength is established along the length of the channel; the strength of the traps is relatively small near the inlet and increases incrementally in the direction of the outlet.

Equation 1 shows that the electrophoretic force depends on the strength of the applied field; however, the dielectrophoretic force depends on both the magnitude and gradient of the local field. More importantly, the electrophoretic force experienced by a particle is a linear function of the local field strength, while the dielectrophoretic force is a second-order function. Because of this nonlinear relationship, their relative contributions to particle motion can vary dramatically depending on the local properties of the field. Further insight into the significance of this relationship can be gained through a qualitative assessment of the effects of varying the local field properties. For a system containing a nonuniform field, when the magnitude of the local field is small, the electrophoretic term will typically dominate and particle motion will be governed by electrophoresis. As the magnitude of the field increases, however, the relative force contribution due to the dielectrophoretic term increases at an exponentially faster rate than the electrophoretic term. For the devices described here, the field strength varies by a factor of about 10 between the first and last 'gate' (set of aligned teeth), whereas the slope of the field squared varies by a factor or about 65. Consequently, if the strength of the field becomes sufficiently large the magnitude of the dielectrophoretic term will become greater than the electrophoretic term and particle motion will be governed by DEP rather than electrophoresis.

In addition to their dependence on local field properties, the interplay between these forces, as well as the magnitude of their effects, is extremely sensitive to even slight differences between particles. The effective electrophoretic and dielectrophoretic forces acting on a particle are determined by its specific physiochemical makeup; their strength depends on a rich set of properties including particle size, morphology, conductivity, and charge distribution.[21,24,25,30,34,36,39] Because of this, the exact field strength and nonuniformity at which a particle's motion becomes governed by dielectrophoretic forces rather than electrophoretic forces will be a unique value determined by the specific structural and chemical properties of the particle. The devices were designed to produce spatially resolved separations by exploiting the characteristic value of field strength and nonuniformity at which the electrophoretic and dielectrophoretic forces acting on a particle are balanced. If the electrophoretic force a particle experiences at a local field maximum is greater than the dielectrophoretic force, the particle will pass by that trap and continue through the channel. When the particle reaches a trap of sufficient strength such that the dielectrophoretic force it experiences as it approaches the local field maximum becomes greater than the electrophoretic forces, the particle will become immobilized, or trapped. It should be noted that in this system particle transport is also affected by electroosmosis. Thus, at the point of isolation all three transport process (electrophoresis, DEP, and electroosmosis) are balanced.

Based on fundamental electrophoretic and dielectrophoretic behaviors, several basic predictions can be made about particle trapping within this system. In general, the greater the difference between the conductivities of the particle and medium, the greater the DEP force experienced by the particle, and the smaller the field gradient needed to support DEP transport. Therefore, in this system, particles that experience a large DEP force should be isolated first, in the relatively weak field gradient traps located close to the inlet. In contrast, particles that experience a small DEP force would require a larger magnitude field gradient and thus should be isolated in the stronger traps located closer to the outlet. Accordingly, these particles are isolated in the stronger traps located closer to the outlet.

Demonstration of the Technique. Separation of live and dead *Bacillus subtilis* cells were obtained using the channel A design (see Experimental Section) (Figure 2, box and image A). The cells were stained using a standard two-color fluorescence assay (SYTO 9 and propidium iodide) by which live and dead cells are stained green and red, respectively. An aliquot of the cell mixture was electrokinetically injected into the channel by applying voltage (1 kV, 200 V/cm) to electrodes located in the sample and outlet reservoirs. The live cells were isolated first, in the weaker DEP

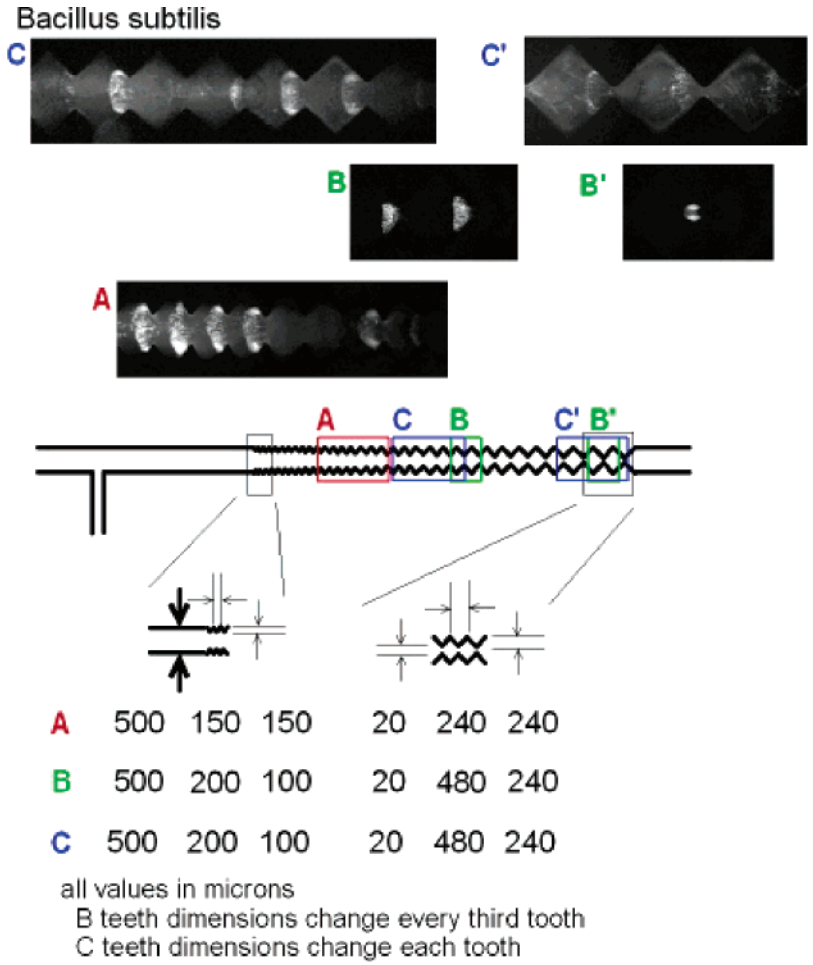

Figure 2. A representative separation of live and dead *Bacillus subtilis* cells obtained using three different channel designs (A, B, and C, see Experimental Section). The direction of flow is left to right (inlet to outlet). In all images, the live cells were isolated on the left, or inlet side of the channel, while the dead cells traveled further down the channel before they were isolated. The cells were stained using a standard two-color fluorescence assay (SYTO 9 and propidium iodide), which stains live cells green and dead cells red, then resuspended in 1 mM phosphate buffer pH 7.6. Images generated for channel A were from an applied electric field of 200 V/cm that was generated via electrodes located in the inlet and outlet reservoirs. Using channel B, a relatively large distance between the two trapping regions resulted in separate images for the live (B) and dead (B′) cells. An outline of a portion of the channel with the location of the images is noted for reference. Also a representative separation of live and dead *Bacillus subtilis* cells obtained using channel C (images and boxes C and C′). The trapping pattern observed for the live cells indicates the existence of distinct subpopulations within the grouping of live cells.

traps, and the dead cells were isolated later, in the stronger DEP traps. The properties of the live and dead cells resulted in a resolved, spatial separation of the two populations. Additionally, we found that the location of the isolated cells and the spatial resolution could be readily adjusting by altering the applied voltage (data not shown).

We investigated two other device designs to assess the effects of altering the spacing and height of the constrictions (Figure 2, boxes and images B, B′, C, and C′). The separation shown in Figure 2, images B and B′ was obtained using channel B (see Experimental Section). The significant differences between channels B and A are that the teeth in channel B are twice as wide at their base, and their heights (base to tip) are in 5 μm increments in channel B as opposed to 10 μm increments in channel A. In both designs, the incremental increases in heights occur after every third tooth in the series. As before, the live and dead cells were isolated in different trapping regions and a spatially resolved separation was obtained; the live cells were trapped first. In this case a much larger spatial separation was observed between the isolated live and dead populations. The difference in spatial resolution can be examined by comparing the physical parameters of the two channels. Increasing the distance between successive trapping regions will increase the spatial resolution of the separation, or in this system the physical distance observed between the isolated populations. The teeth in channel B are wider than those in channel A; thus, the tips of the teeth and their corresponding field maxima are spaced farther apart. Additionally, because the heights of the teeth in channel B increase in smaller increments, the entire series of electric field gradients is distributed across a longer distance. Therefore, the spatial resolution of the separations should be greater in channel B.

Another separation of *Bacillus subtilis* was obtained using channel C (see Experimental Section) (Figure 2, images and boxes C and C′). As in channel B, the bases of the teeth are wider than those in channel A. Their heights increase in 5 μm increments as well; however, in this channel the increase occurs after each tooth in the series rather than after every third. The distribution must to be due to differences in the properties of the cell populations

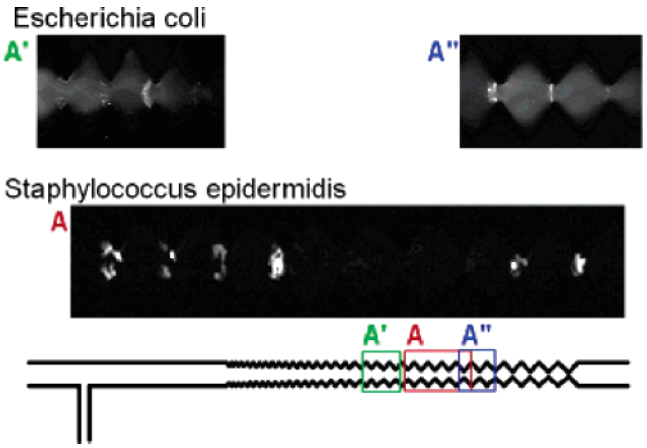

Figure 3. A representative separation of live and dead *Escherichia coli* cells obtained using channel A. The direction of flow is left to right (inlet to outlet). The live cells were isolated first (shown on the left, or inlet side of the channel), while the dead cells traveled further down the channel before they were isolated. All experimental conditions are the same as those for Figure 2 except the strength of the applied field is 300 V/cm. Also shown is representative separation of live and dead *Staphylococcus epidermidis* cells (image and boxes A′ and A″) obtained using channel A. The direction of flow is left to right (inlet to outlet). All experimental conditions are the same as those in Figure 2.

isolated in the different traps. Previous studies have shown that the dielectric properties of cell membranes are dynamic in nature, reflecting such factors as environment, growth, and disease state.[23,24,29,31,34,38,39,52,53] Thus, it is reasonable to suggest that the trapping pattern and apparent subpopulations observed here may also represent different growth or developmental states of the cells. However, further studies will be needed to fully investigate and characterize the specific properties of these populations. A detailed explanation for the relative distribution of *Bacillus subtilis* throughout each of these three devices will have to await a detailed understand of both the separatory mechanism and the response of this mechanism to the various physical and chemical properties of living and dead cells.

To assess the versatility of the technique, we performed comparable studies using various other species of bacteria: live and dead *Esherichia coli* and *Staphylococcus epidermidis* cells (Figure 3). Spatially resolved separations were obtained for all of the species studied. The live and dead cell populations were isolated in the same order as before; however, both the location of trapping and the required voltage differed. These results indicate the technique is quite flexible and suggest that it can be applied to different biological particles and structures, as well as more complex mixtures.

The device presented here offers several benefits, even though it is only meant as a proof-of-principle demonstration. First, unlike many DEP based devices, it is not inherently limited to separating two distinctly different components. Both the spatial resolution and the difference in magnitude of the successive traps can be controlled by altering the physical parameters of the channels. Furthermore, this design flexibility allows for adjustments to accommodate the specific range of desired capture properties of a given application or range of particle sizes or cell populations. Second, because electrophoresis and electroosmosis are incorporated, the process does not rely on diffuse transport; therefore, separations occur very rapidly. Third, two sample introduction methods are possible. A small aliquot of the sample can be injected as described in this work, or the sample can be continuously fed into the channel. Fourth, the separation remains stable as long as the field is applied; therefore, the technique can be run for as long as needed to collect the necessary quantity of particles. This aspect of the technique may be especially conducive to integration of detection methods.

Model System Capture Order. In the presence of a low frequency or DC electric field, biological membranes behave like very low loss capacitors, blocking electric fields and current from the interior of the cell.[18,24,34,49,52] Conceivably, because of this DC current blocking effect, the general dielectrophoretic response of a cell to a nonuniform DC field depends on the conductivity of its membrane rather than the properties of its internal components. The specific conductivity of a cell membrane is a function of various properties, most notably the membrane components, and the viability or growth state of the cell. A typical live bacteria cell has a very low membrane conductivity ($\sim 1 \times 10^{-4,}$ $\sim\mu$S/mm); however, upon death, its membrane becomes permeable, leading to a drastic increase in conductivity ($\sim 1\ \mu$S/mm). In either case, the membrane conductivity is lower than that of an aqueous medium or buffer, which would necessarily have a conductivity equal to or greater than that of DI water ($\sim 2.25\ \mu$S/mm). For that reason, both the live and the dead cells will undergo negative DEP in the presence of a nonuniform DC electric field. Additionally, the live cells, being much less conductive than the dead ones, will experience greater dielectrophoretic forces. Therefore, live cells in general will trap before the dead ones under these conditions.

CONCLUSIONS

We have developed a new DC-iDEP device for separating biological particles and structures. This structure produces sequential, spatially resolved separations in devices containing a series of progressively stronger field gradient regions distributed along the length of the channel. The particles are initially transported through the channel by electrophoretic transport mechanisms and then isolated according to their characteristic electrophoretic and dielectrophoretic properties. In this work, we described the technique theoretically and demonstrated proof-of-principle using bacteria cells as the model system for biological structures. The promising results obtained in this preliminary work suggest the technique may form the basis of a highly versatile and useful tool for separating biological particles. Future studies will focus on achieving greater control over resolution and expanding its application to a wide variety of particles and structures.

ACKNOWLEDGMENT

This work was supported by Arizona Applied NanoSensors.

Received for review March 15, 2007. Accepted April 3, 2007.

AC070534J

(52) Burt, J. P. H.; Pethig, R.; Gascoyne, P. R. C.; Becker, F. F. *Biochim. Biophys. Acta* **1990**, *1034*, 93−101.
(53) Yang, J.; Huang, Y.; Wang, X. B.; Becker, F. F.; Gascoyne, P. R. C. *Biophys. J.* **2000**, *78*, 2680−2689.